TOWARDS NONLINEAR MODELING OF THE COMBINED SEXTUPOLE-CORRECTOR MAGNETS AT SOLEIL II

Z. Zhang*, A. Loulergue, F. Marteau, T. Mutin, L. S. Nadolski, V. Pinty
Synchrotron SOLEIL, Saint-Aubin, France

Abstract

The SOLEIL II sextupoles are equipped with additional windings to provide normal and skew dipole corrections. Accurate modeling of these combined-function sextupole magnets are particularly challenging due to magnetic saturation, hysteresis, and internal cross-talk between channels. Based on 3D magnetic simulations, polynomial, interpolation-based, and neural-network models were developed to reproduce the saturation and cross-talk effects. These nonlinear models were validated on the first prototype magnet, providing preliminary confirmation of their reliability and demonstrating the feasibility of implementing sextupole-corrector magnets in the SOLEIL II storage ring.

INTRODUCTION

The SOLEIL II project is an upgrade of the SOLEIL synchrotron light source based on the design of a new storage ring with compact, high-gradient magnetic elements [1–7]. In this context, sextupoles are equipped with additional windings for orbit correction. These magnets feature three independent control channels, corresponding to the main sextupole current I_{sx}, the horizontal corrector current I_{ch}, and the vertical corrector current I_{cv}. Their combination enables the generation of specific multipole components, namely a skew dipole a_1, a normal dipole b_1, and a normal sextupole b_3.

Accurate nonlinear modeling of these magnets is essential for the reliable control of both the main and corrector power supplies in storage ring operation. To define the required modeling precision, the impact of sextupole field errors on the dynamic aperture (DA) and the Touschek lifetime was evaluated using random field perturbations applied to all sextupoles in the SOLEIL II lattice. Based on the results summarized in Table 1, a preliminary target relative error (RE) for the sextupole field is set to within ±0.1 %. In addition, considering the impact of corrector errors on the orbit feedback system, the allowable absolute error (AE) of the corrector kick is typically limited to 1 µrad.

Table 1: Sextupole Field Error Impact

SX Strength max. RE	**±0.1 %**	**±0.5 %**
Relative DA impact	Marginal	Weak
Relative Touschek lifetime drop	~−4 %	~−20 %

Twelve types of combined-function sextupole magnets have been designed for SOLEIL II [8, 9]. Nonlinear modeling was first performed on a standard sextupole (length: 90 mm, diameter: 16 mm, gap: 6.2 mm). Based on 3D magnetic simulations using Opera/Tosca [10], the magnetic saturation becomes evident when the main current exceeds 40 A, as shown in Fig. 1. Furthermore, due to internal cross-talk with the dipole correction channels, the integrated sextupole strength at maximum current (50 A) is reduced by approximately 5 %, as illustrated in Fig. 2.

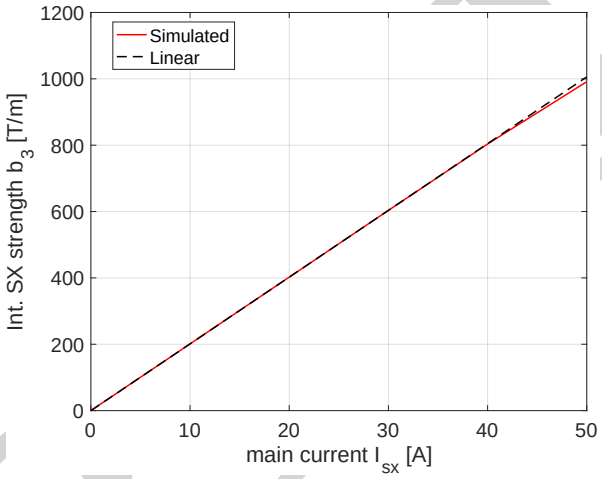

Figure 1: Integrated sextupole strength versus main current, with horizontal and vertical corrector currents set to zero.

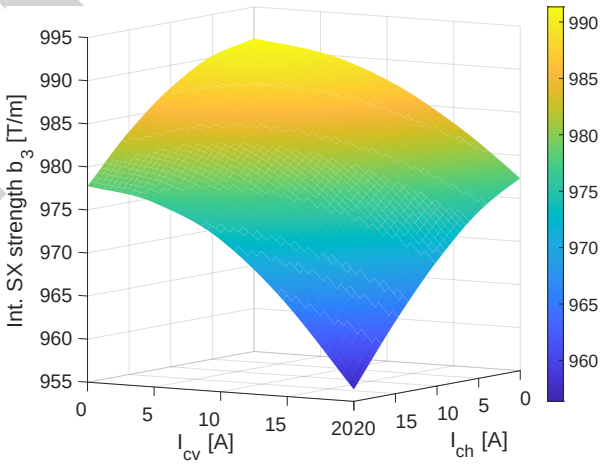

Figure 2: Integrated sextupole strength at a main current of 50 A versus horizontal and vertical corrector currents.

At this preliminary stage, hysteresis effects are not yet considered. The nonlinear modeling of saturation and cross-talk effects in the combined sextupole-corrector magnets is performed using three types of models: polynomial, interpolation-based, and neural-network models. These models are described and compared in this paper, followed by validation against measurements on the first prototype.

* zhandong.zhang@synchrotron-soleil.fr

NONLINEAR MODELING

Polynomial Model

As a first step, polynomial modeling was investigated to describe the nonlinear behavior of the sextupole-corrector magnets [11]. In this model, the three magnetic field components a_1, b_1, and b_3 are expressed as nonlinear functions of I_{sx}, I_{ch}, and I_{cv}. After testing formulations with orders ranging from one to six, the fourth-order model was found to provide the best compromise between fitting accuracy and model complexity. The complete polynomial basis includes linear, quadratic, cubic, quartic, and mixed cross terms between the current channels. The resulting model contains 35 polynomial coefficients and can be written in matrix form as $a_1 = \mathbf{X} \cdot c_{a_1}$, $b_1 = \mathbf{X} \cdot c_{b_1}$, and $b_3 = \mathbf{X} \cdot c_{b_3}$, where $\mathbf{X}$ is the design matrix composed of the polynomial basis functions, and c_{a_1}, c_{b_1}, c_{b_3} denote the corresponding coefficient vectors. The coefficients were obtained from the simulation data through least-squares regression using the pseudo-inverse of $\mathbf{X}$.

The I_{sx} values of the magnetic simulation data used for the fitting range from 0 to 50 A with a step of 10 A, while I_{ch} and I_{cv} range from 0 to 20 A with a step of 5 A. The modeling performance summarized in Table 2 was characterized in terms of the maximum AE of kicks generated by a_1 and b_1, together with the maximum RE of b_3 (the RE calculated only for field values exceeding 1 % of the maximum b_3 field). The predictive performance was estimated using additional magnetic simulation data at saturated operating points with $I_{sx} = 45$ A. Using the polynomial model, a fitting RE of up to 0.78 % was obtained for the b_3 component. Compared with the 0.1 % accuracy target required for machine operation, the polynomial model was therefore considered insufficiently accurate.

Interpolation-based Model

The second approach consists of an interpolation-based model constructed directly from the simulation data. The data were first organized on a regular grid defined by I_{sx}, I_{ch}, and I_{cv}. The corresponding magnetic field components were then reshaped into three-dimensional arrays and reordered to match the grid structure. Based on this gridded dataset, three independent interpolating functions were constructed using a spline-based gridded interpolation method. The resulting models provide continuous representations of the magnetic field components over the full operating range of the three input currents.

The predictive performance of these interpolators, as summarized in Table 2, is superior to that of the polynomial model when evaluated using the same performance criteria. However, the maximum predictive RE of b_3 still reaches 0.22 %, which remains above the required accuracy target.

Neural-network Model

To simultaneously achieve the required fitting and predictive accuracy, a neural-network approach was further investigated. Three independent neural networks were trained separately for a_1, b_1, and b_3 to mitigate cross-talk effects. The training was performed using the Bayesian regularization backpropagation algorithm [12, 13] in order to improve generalization capability and reduce overfitting. To reduce the dependence on random initialization, 100 independent trainings were carried out for each magnetic field component. The network providing the lowest maximum RE was selected as the final model.

To determine the optimal network architecture, neural networks with one, two, and three hidden layers were investigated. For each configuration, the number of neurons in each hidden layer, as well as the proportions of the training, validation, and testing subsets, were further optimized. Considering both the accuracy and the overall model complexity, the two-hidden-layer network was selected as the optimal solution at the current stage.

The modeling performance of the neural-network models is shown in the last row of Table 2. The maximum fitting and predictive REs obtained for b_3 are 0.02 % and 0.09 %, respectively, satisfying the preliminary precision requirement for preserving the Touschek lifetime of the storage ring.

FIRST PROTOTYPE MEASUREMENTS

The first prototype of the SOLEIL II sextupole-corrector magnet was delivered to SOLEIL in October 2023. This prototype (length: 80 mm, diameter: 16 mm, gap: 7.5 mm), featuring a notched design, exhibits significant saturation and cross-talk effects, as indicated by preliminary measurements [14]. Successful validation of the three nonlinear modeling approaches on this prototype would provide strong confidence in their applicability to other types of combined-function sextupole magnets designed for SOLEIL II.

Dedicated measurements for model validation were performed using a stretched wire bench [15], with motion control, power-supply regulation of the three current channels, and data acquisition interfaced with Igor Pro [16]. To minimize hysteresis effects, the sextupole was cycled before each magnetic field measurement, and demagnetized prior to each change in current setting. To improve measurement precision, five measurements were performed at each current setting, and their mean value was taken as the final result, with a maximum standard deviation of 3.4×10^{-4} T observed across the repetitions.

The current settings used in the first measurement followed the same points as those used in the simulation dataset for model fitting. Additional measurements performed at a main current of 45 A were used to evaluate the predictive performance. The modeling performances of the three nonlinear approaches validated against magnetic measurements are presented in the first, third, and fifth rows of Table 3, respectively, with no significant degradation compared with those estimated from simulation data.

Since the maximum predictive RE of b_3 obtained with both the interpolation-based and neural-network models remained close to, but slightly above, the required accuracy target, an additional study was carried out to investigate

Table 2: Estimated Modeling Performance from Simulation Data

Model	Fitting performance			Predictive performance		
	a_1 max. AE	b_1 max. AE	b_3 max. RE	a_1 max. AE	b_1 max. AE	b_3 max. RE
Polynomial	11 µrad	5 µrad	0.78 %	10 µrad	8 µrad	0.32 %
Interpolation-based	–	–	–	4 µrad	5 µrad	0.22 %
Neural-network	0.03 µrad	0.3 µrad	0.02 %	7 µrad	2 µrad	0.09 %

Table 3: Validated and Optimized Modeling Performance against Measurements on the First Prototype

Model	Fitting performance			Predictive performance		
	a_1 max. AE	b_1 max. AE	b_3 max. RE	a_1 max. AE	b_1 max. AE	b_3 max. RE
Polynomial	19 µrad	10 µrad	0.91 %	11 µrad	12 µrad	0.51 %
	(29 µrad)	(13 µrad)	(1.11 %)	(6 µrad)	(10 µrad)	(0.16 %)
Interpolation-based	–	–	–	3 µrad	6 µrad	0.21 %
	–	–	–	(12 µrad)	(3 µrad)	(0.08 %)
Neural-network	0.05 µrad	0.2 µrad	0.03 %	9 µrad	5 µrad	0.13 %
	(0.2 µrad)	(0.5 µrad)	(0.03 %)	(11 µrad)	(3 µrad)	(0.06 %)

the effect of increasing the fitting data size. The density of the measuring points was therefore doubled by reducing the main current step from 10 A to 5 A. The predictive performance was tested using additional measured data at saturated operating points with the main current set to 47.5 A. The optimized results are shown in brackets in the second, fourth, and sixth rows of Table 3. The maximum predictive RE of the interpolation-based model was reduced from 0.21 % to 0.08 %, while that of the neural-network model decreased from 0.13 % to 0.06 %. These results demonstrate both the improvement capability of the proposed modeling approaches with increased data density and their ability to achieve the required accuracy for the sextupole strength within the saturation region.

For the two dipole components a_1 and b_1, the predictive AEs of their kicks exceed the target limit of 1 µrad, both in Table 2 and Table 3. This is likely related to the absence of simulation and measurement data for negative corrector currents, leading to reduced fitting stability near points with $I_{ch} = 0$ or $I_{cv} = 0$. Further studies, including extending the ranges of I_{ch} and I_{cv} to negative values and increasing the density of the dataset, are planned to improve the modeling performance for a_1 and b_1.

SUMMARY AND OUTLOOK

To ensure proper operation of the combined sextupole-correctors in the SOLEIL II storage ring, preliminary studies on nonlinear modeling were carried out to reproduce their saturation and internal cross-talk effects. The performance of the three modeling approaches was first evaluated using magnetic simulation data and subsequently validated against measurements from the first prototype, demonstrating their capability to meet the required accuracy in sextupole strength.

In the next steps, besides further improving the modeling performance for the two dipole components, the inverse modeling procedure, from magnetic field strengths to current settings, will be investigated in terms of both precision and response speed. In addition, hysteresis modeling will be initiated based on dedicated measurements of the first prototype. Finally, a hybrid model combining all relevant nonlinear effects will be developed.

REFERENCES

[1] Synchrotron SOLEIL Facility Website, https://www.synchrotron-soleil.fr

[2] Conceptual Design Report for the SOLEIL Upgrade, https://www.synchrotron-soleil.fr/en/future-soleil-soleil-ii-project

[3] A. Nadji and L. S. Nadolski, "Upgrade project of the SOLEIL accelerator complex", *Synchrotron Radiat. News*, vol. 36, no. 1, pp. 10–15, 2023. doi:10.1080/08940886.2023.2186661

[4] J. Susini *et al.*, "A brief introduction to the Synchrotron SOLEIL and its upgrade programme", *Eur. Phys. J. Plus*, vol. 139, no. 80, 2024. doi:10.1140/epjp/s13360-024-04872-2

[5] A. Loulergue *et al.*, "TDR baseline lattice for SOLEIL II upgrade project", in *Proc. IPAC'24*, Nashville, TN, Jul. 2024. doi:10.18429/JACoW-IPAC2024-TUPG47

[6] L. S. Nadolski *et al.*, "SOLEIL II project: entrance in the construction phase", in *Proc. IPAC'25*, Taipei, Taiwan, Jun. 2025, pp. 212–215. doi:10.18429/JACoW-IPAC2025-MOPB074

[7] L. S. Nadolski *et al.*, "SOLEIL II: the French 4GLS project - first year of the construction program", presented at IPAC'26, Deauville, France, May 2026, paper TUO2M01, this conference.

[8] C. Kitegi *et al.*, "Magnet design status of SOLEIL II", *IEEE Transactions on Applied Superconductivity*, vol. 34, no. 5, pp. 1–5, 2024. doi:10.1109/TASC.2024.3375294

[9] A. Ouazib *et al.*, "The SOLEIL II magnets", presented at IPAC'26, Deauville, France, May 2026, paper MOP7059, this conference.

[10] Opera, Dassault Systèmes. https://www.3ds.com/products/simulia/opera

[11] G. Le Bec, "A fast non-linear model for the EBS combined sextupole-corrector magnets", in *Proc. IPAC'21*, Campinas, SP, Brazil, pp. 2381–2383, Aug. 2021. doi:10.18429/JACoW-IPAC2021-TUPAB369

[12] D. J. C. MacKay, "Bayesian interpolation", *Neural Computation*, vol. 4, no. 3, pp. 415–447, 1992. doi:10.1162/neco.1992.4.3.415

[13] F. Dan Foresee and M. T. Hagan, "Gauss-Newton approximation to Bayesian learning", in *Proc. ICNN'97*, vol. 3, Houston, TX, pp. 1930–1935, Jun. 1997. doi:10.1109/ICNN.1997.614194

[14] C. Kitegi, "Magnets for SOLEIL II", in *23rd International Magnetic Measurement Workshop*, Bad Zurzach, Switzerland, Oct. 2024. https://indico.psi.ch/event/15256/contributions/52546/

[15] G. Le Bec, J. Chavanne, and Ch. Penel, "Stretched wire measurement of multipole accelerator magnets", *Phys. Rev. ST Accel. Beams*, vol. 15, no. 2, p. 022401, 2012. doi:10.1103/PhysRevSTAB.15.022401

[16] Igor Pro, WaveMetrics, Inc. https://www.wavemetrics.com